

Orbital Josephson effect and interactions in driven atom condensates

M. Heimsoth,^{1,2} C. E. Creffield,¹ L. D. Carr,^{2,3} and F. Sols¹

¹*Departamento de Física de Materiales, Universidad Complutense de Madrid, 28040 Madrid, Spain*

²*Department of Physics, Colorado School of Mines, Golden, Colorado 80401, USA*

³*Physikalisches Institut, Universität Heidelberg, Philosophenweg 12, 69120 Heidelberg, Germany*

(Dated: March 13, 2019)

In a system of ac-driven condensed bosons we study a new type of Josephson effect occurring between Floquet states sharing the same region of space and the same internal atom structure. We first develop a technique to calculate the long time dynamics of a driven interacting many-body system. For resonant frequencies, this dynamics can be derived from an effective Hamiltonian whose operators satisfy standard commutation rules. Within the subspace of resonant states, a locally repulsive interaction between bosons translates into an effective attraction. We apply the method to study the effect of interactions on the coherent ratchet current of an asymmetrically driven boson system. We find a wealth of dynamical regimes which includes Rabi oscillations, self-trapping, and chaotic behavior.

PACS numbers: 03.75.Lm, 67.85.De

The Josephson effect (JE) is a fundamental quantum phenomenon which reflects the coherent occupation of two, or a few, single-particle states by a macroscopic number of bosons. It was first predicted [1] and observed [2] for superconductors, and seen later in superfluids [3]. In Bose-Einstein condensates (BECs) one may refer to the internal or external JE, depending on whether the two coherently connected states occupy the same region of space with different internal atomic states, or two different regions with the same spin state. Both the internal [4, 5] and the external [6] JE have been observed. The internal JE holds the promise of generating highly entangled quantum many-body systems [7]. Here we report on a new type of JE which involves the macroscopic coherent occupation of Floquet states in ac-driven BECs. This *orbital Josephson effect* is properly neither external nor internal, since the connected Floquet states occupy the same region of space with the same internal atom structure, their sole difference residing in their orbital state.

The Josephson effect requires interactions to display truly collective behavior associated with the macroscopic occupation of two states [8, 9]. In the absence of interactions, the resulting Rabi dynamics is merely an amplification of the dynamics undergone by a single atom [4, 9]. The study of interactions in ac-driven many-body systems has been generally restricted to either a two-mode approximation [10], or to mean field approaches in bosonic ensembles [11–13]. Here we develop a description of the coarse-grained dynamics of the quantum field operator in an ac-driven many-boson system, thus going beyond a mean-field treatment and its first corrections. We find that, in the case of resonantly connected Floquet states, the long-time evolution can be described by conventional quantum dynamics, by which we mean deriving from an effective interacting Hamiltonian. If the driving provides the only external potential, we find that a repulsive interaction in real space translates into an at-

tractive interaction in the truncated Hilbert space of a discrete number of resonantly connected Floquet states. We apply these findings to understand in depth the role of interactions in asymmetrically driven BECs which exhibit the quantum ratchet effect [11, 12, 14, 15], together with a wealth of dynamic regimes.

Our starting point is the equation of motion for the field operator of a system of interacting bosons,

$$i\partial_t\hat{\psi}(x,t) = [H(x,t) + \lambda\hat{\psi}^\dagger\hat{\psi}]\hat{\psi}(x,t). \quad (1)$$

where $H(x,t) = -\frac{1}{2}\partial_{xx} + V(x,t)$ includes a time-dependent potential, and λ is the effective strength of the contact interaction in a quasi-one-dimensional ring of radius R . We set $\hbar = 1$ and measure all energies and frequencies in units of \hbar^2/MR^2 , with M the atomic mass. Furthermore, our unit of length is R , so that the circumference of the ring is 2π . Such rings, as schematically depicted in Fig. 1a, have been experimentally realized (e.g. [16]). The field operator $\hat{\psi}(x,t)$ obeys periodic boundary conditions in x , and its algebraic structure is given by the standard equal-time bosonic commutation relations: $[\hat{\psi}(x_1,t), \hat{\psi}^\dagger(x_2,t)] = \delta(x_1 - x_2)$ and $[\hat{\psi}(x_1,t), \hat{\psi}(x_2,t)] = 0$.

In order to study the coarse-grained, long-time dynamics of the many-body system, we generalize the (t, t') for-



FIG. 1. *Schematics of the orbital Josephson effect.* (a) Resonant driving induces coupling between the zero-momentum and two opposite momentum eigenmodes. The resulting Josephson link between these orbitals, with Rabi frequencies Γ_{\pm} , has a negative effective interaction energy. (b) A possible departure from exact resonance lifts the degeneracy of the quasi-energies.

malism originally developed for single particles [17] and note that $\hat{\psi}(x, t)$ can be obtained as

$$\hat{\psi}(x, t) = \hat{\psi}(x, t'; t)|_{t'=t}, \quad (2)$$

provided $\hat{\psi}(x, t'; t)$ satisfies

$$i\partial_t \hat{\psi}(x, t'; t) = [H(x, t') - i\partial_{t'} + \lambda \hat{\psi}^\dagger \hat{\psi}] \hat{\psi}(x, t'; t) \quad (3)$$

together with the commutation relations $[\hat{\psi}(x_1, t'; t), \hat{\psi}(x_2, t'; t)] = \delta(x_1 - x_2)$, which are needed to obtain the standard commutation relations for $\hat{\psi}(x, t)$ through the prescription (2).

To include the effect of a weak time-periodic perturbation, $V(x, t) = V(x, t + T)$, it is convenient to work in the representation of unperturbed ($V = 0$) Floquet states. The first-quantized version of (3) was studied in Ref. 14 in the absence of interactions. The unperturbed stationary states evolve as

$$\psi_{\ell m}(x, t'; t) = \phi_{\ell m}(x, t') \exp(-i\varepsilon_{\ell m}^0 t), \quad (4)$$

where ℓ, m are integers and represent momentum and canonical conjugate of the t' variable, and

$$\phi_{\ell m}(x, t') = \frac{1}{\sqrt{2\pi}} \exp(i\ell x - im\omega t'), \quad (5)$$

is the wave function of unperturbed ($V = 0$) Floquet state with quasi-energy $\varepsilon_{\ell m}^0 = \frac{1}{2}\ell^2 - m\omega$, with $\omega = 2\pi/T$. The operators in this representation,

$$\hat{a}_{\ell m}(t) = \frac{1}{T} \iint dx dt' \phi_{\ell m}^*(x, t') \hat{\psi}(x, t'; t), \quad (6)$$

satisfy the equation of motion

$$i\partial_t \hat{a}_{\ell m} = \varepsilon_{\ell m}^0 \hat{a}_{\ell m} + \sum_{\ell' m'} V_{\ell m, \ell' m'} \hat{a}_{\ell' m'} + \frac{\lambda}{2\pi} \sum_{\ell' m' \ell'' m''} \hat{a}_{\ell' m'}^\dagger \hat{a}_{\ell'' m''} \hat{a}_{\ell' - \ell'' + \ell, m' - m'' + m}, \quad (7)$$

with the unconventional commutation relations

$$\sum_{m'} [\hat{a}_{\ell, m+m'}(t), \hat{a}_{\ell' m'}^\dagger(t)] = \delta_{\ell \ell'} \delta_{m0}. \quad (8)$$

Here $V_{\ell m, \ell' m'}$ is the matrix element of the driving operator between two unperturbed states such as (4). When the driving frequency is such that the system is at or close to resonance, only a few states (all with the same or similar value of $\varepsilon_{\ell m}^0$) are relevant [11, 12, 14]. Importantly, in that subspace the index m is uniquely determined by ℓ . Thus within that truncated space we can drop the index m . As a result, (8) becomes equivalent to the standard commutation relations $[\hat{a}_\ell(t), \hat{a}_{\ell'}^\dagger(t)] = \delta_{\ell \ell'}$.

If we calculate the effective matrix elements connecting the various resonant unperturbed Floquet states, we are left with a conventional few-mode boson problem

whose dynamics, given by (7), can be studied using established techniques. The resulting dynamics between Floquet states reflects the coarse-grained, long-time dynamics of the true quantum state evolution.

Within the degeneracy subspace, where conventional commutation relations apply, Eq. (7) can be viewed as a Heisenberg equation deriving from the interacting many-body Hamiltonian

$$\hat{H} = \sum_{\ell} \varepsilon_{\ell}^0 \hat{n}_{\ell} + \sum_{\ell \ell'} \Gamma_{\ell \ell'} \hat{a}_{\ell}^\dagger \hat{a}_{\ell'} + \frac{\lambda}{4\pi} \sum_{\ell \ell'} \sum_{\ell''} \hat{a}_{\ell+\ell''}^\dagger \hat{a}_{\ell'-\ell''}^\dagger \hat{a}_{\ell} \hat{a}_{\ell'}, \quad (9)$$

where $\Gamma_{\ell \ell'}$ may allow for second-order processes between resonant states mediated by a non-resonant state [14], $\hat{n}_{\ell} = \hat{a}_{\ell}^\dagger \hat{a}_{\ell}$ is the occupation of state ℓ , and ℓ'' can only take values 0 or $\ell' - \ell$ if $\ell \neq \ell'$, and 0 if $\ell = \ell'$.

The conservation of total particle number $\sum_{\ell} \hat{n}_{\ell}$ leads to the interesting result that, up to a constant, the Hamiltonian (9) is equivalent to

$$\hat{H} = \sum_{\ell} \varepsilon_{\ell}^0 \hat{n}_{\ell} + \sum_{\ell \ell'} \Gamma_{\ell \ell'} \hat{a}_{\ell}^\dagger \hat{a}_{\ell'} - \frac{\lambda}{4\pi} \sum_{\ell} \hat{n}_{\ell}^2. \quad (10)$$

Thus a *repulsive* interaction in real space translates into an *attractive* interaction in momentum space. The resulting energy gain in the macroscopic occupation of a single state in gases with repulsive interactions underlies the stability of Bose-Einstein condensation as discussed in Ref. 18.

To derive (10), we have used the selection rules (stemming from the simultaneous conservation of momentum and quasi-energy) which are implicit in Eqs. (7)-(9). Interestingly, in those dynamical regimes where the truncated resonant space is effectively reduced to two modes, Eq. (10) applies for orbitals of arbitrary shape (not necessarily plane waves), but with an interaction strength that is state dependent.

When a few modes are macroscopically occupied, Eq. (9) describes a Josephson-type link between states $\ell \ell'$ with Rabi frequency $\Gamma_{\ell \ell'}$. Remarkably, this Josephson link takes place between atom states with the same internal state and occupying the same region of space. Thus it is not appropriate to describe it as an internal or external JE. The Hamiltonian (10) describes what can be termed the orbital Josephson effect, which here occurs between resonant Floquet states in ac-driven Bose condensates.

As a particular application of the method developed here to treat the many-body problem in driven systems, we consider a BEC subject to the asymmetric driving

$$V(x, t) = K [\sin(kx) + \alpha \sin(2kx + \varphi)] [\sin(\omega t) + \beta \sin(2\omega t)],$$

which has been numerically studied [12] and experimentally implemented [19]. For $\varphi \neq \frac{1}{2}\pi, \frac{3}{2}\pi$ it yields a coherent quantum ratchet provided that both α and β are nonzero.

We consider a system initially prepared in $|\ell\rangle = |0\rangle$. It was analytically shown in Ref. 14 that, if we drive it with resonant frequency $\omega = 1$ and small amplitude K , the subsequent evolution will mix the initial state only with the states $|\ell\rangle = |\pm 2\rangle$. These three states all satisfy the resonance condition $\varepsilon_\ell^0 = 0$, and we label them with the indices $\pm, 0$. The resulting three-level-system Hamiltonian is

$$\hat{H}_{3\text{LS}} = \Gamma_+ \hat{a}_+^\dagger \hat{a}_0 + \Gamma_- \hat{a}_-^\dagger \hat{a}_0 + \text{H.c.} - \frac{\lambda}{4\pi} \sum_\nu \hat{n}_\nu^2 - 2\Delta(\hat{n}_+ + \hat{n}_-). \quad (11)$$

where ν takes values $\pm, 0$, and $\Delta = \omega - 1$ accounts for a possible small detuning that shifts the quasi-energies in (10) to $\varepsilon_\ell^0 = -(\ell^2/2)\Delta$. Near resonance the tunneling parameters Γ_\pm can be calculated analytically [14]. For $\Delta \ll 1$, one finds

$$\Gamma_\pm = \frac{K}{4} \left(\frac{K}{2} \pm \alpha\beta e^{\pm i\varphi} \right). \quad (12)$$

This result demonstrates that the quantum ratchet current (which requires $|\Gamma_+| \neq |\Gamma_-|$) originates in the interference between first- and second-order process in the driving strength [14]. In Eq. (12) we have neglected the possible effect of interactions on the tunneling terms. Without interactions, the initial state $|0\rangle$ couples only to a state $|a\rangle$ which is an asymmetric combination of $|\pm\rangle$, yielding an average current which is half that carried by $|a\rangle$ [14]. It has been noticed that interactions destroy the coherent current [12]. Below we study the role of interactions in depth and show that they yield a rich variety of dynamical regimes.

We employ three different approximations to investigate the many-body problem: full numerical resolution of the time-dependent Gross-Pitaevskii equation (FGP) using a Runge-Kutta method; study of the GP equation in the truncated space of the three resonant states $0, \pm$ (3GP); and resolution of the many-body problem in the three-level system (3LS), via exact diagonalization of the effective interacting Hamiltonian (11) with 40 atoms. Importantly, we note that 3GP can be obtained both as a truncation of FGP or a mean-field version of 3LS. We always assume the condensate to be initially in state 0.

Figure 2 shows the expectation value of the ratchet current $\langle I(t) \rangle$ – given by the mean momentum per particle – over the first 200 driving cycles. The regimes of weak, moderate, and strong interaction (as characterized by $g \equiv \lambda N$), are all calculated with the three methods described above. For weak interactions, the two truncated-space calculations (3GP and 3LS) yield similar Rabi oscillations, both differing from FGP in that they do not display high-frequency dynamics, as revealed both in the Fourier spectrum and in the time dependence of the current. The fast dynamics of FGP disappears if the stroboscopic current is plotted, as shown in the shaded region. For strong interactions, the system tends to remain trapped in the initial state, as may be expected

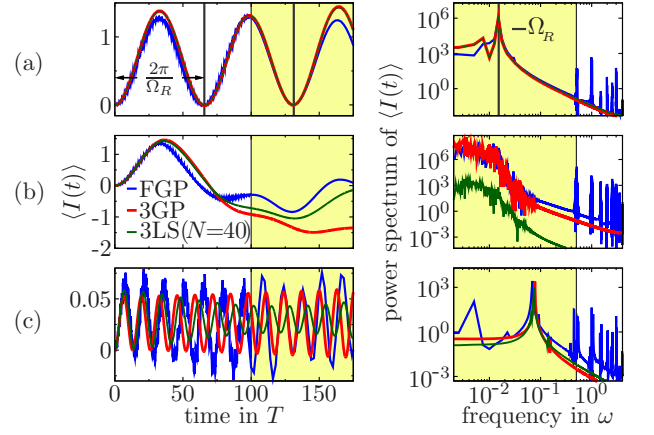


FIG. 2. Time evolution and power spectrum of the particle current. Three regimes are depicted: (a) weak interaction strength ($g=0.01$), showing regular Rabi oscillations; (b) intermediate interaction ($g=0.08$), displaying chaotic dynamics; and (c) strong interaction ($g=0.5$), showing self-trapping. Parameters: $K = 0.2$, $\varphi = 0$, $\omega = 1$ ($\Delta = 0$), $\alpha = \beta = 0.2$. In the shaded region we present the stroboscopic current, which erases the short time dynamics responsible for the peaks in the white region of the current spectrum. Three different calculation methods are employed.

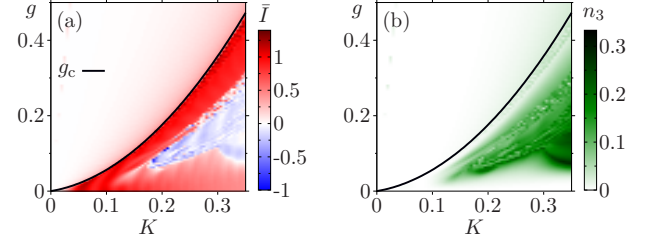


FIG. 3. (a) Continuous time average of the quantum ratchet current at long times (400 driving cycles) for different amplitudes and interaction strength. (b) Third largest eigenvalue of the time-averaged one-body density matrix. Parameters: $\omega = 1$ ($\Delta = 0$), $\alpha = \beta = 0.2$, $K = 0.2$, $\varphi = 0$.

since (11) has the structure of a Josephson link with *negative* interaction energy [20]. The three numerical methods predict differing behaviors of the resulting small current, but agree on the position and strength of the main peak in the spectrum. For intermediate interaction, discrepancies between methods soon appear, which suggests chaotic behavior. This is confirmed and studied further below.

Figure 3a shows the continuous time average of the ratchet current $\bar{I}(t) \equiv t^{-1} \int_0^t dt' \langle I(t') \rangle$ after 400 cycles, computed within 3GP, as a function of g and K at exact resonance. We assume $|\Gamma_+| > |\Gamma_-|$ – see Eq. (12). For small K , the perturbative scheme of [14] applies, and at weak interaction a nonzero ratchet current results from Rabi oscillations between $|0\rangle$ and $|a\rangle$. For stronger interactions the ratchet current disappears, because the system remains in the initial state $|0\rangle$ due to the large

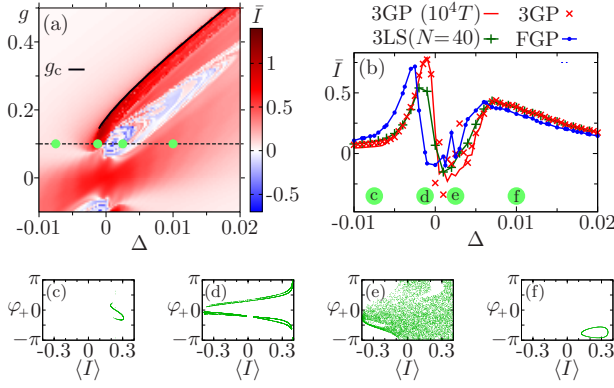


FIG. 4. (a) Quantum ratchet current as a function of the interaction strength and the detuning. The behavior along the dashed line is shown in (b) for four different calculations (3GP is computed at two different times). Poincaré sections are shown for the representative points (c-f), obtained from points in the hyperplane $n_+ + n_- = 0.2$. The plotted variables are the instantaneous ratchet current $\langle I \rangle$ and the relative phase φ_+ between states $|0\rangle$ and $|+\rangle$. Parameters: $\alpha = \beta = 0.2$, $K = 0.2$, $\varphi = 0$. In (a-b) averages are performed over 400 cycles unless otherwise indicated.

negative energy associated with the macroscopic occupation of $|0\rangle$ [see Eq. (10)]. This can be viewed as a form of macroscopic quantum self-trapping [21], albeit with a negative effective interaction energy. We find that just below the critical interaction strength the system oscillates between $|0\rangle$ and $|+\rangle$. This is consistent with the fact that the threshold interaction value obtained from that assumption, $g_c = 8\pi|\Gamma_+|$, agrees well with the numerical simulation (see solid curve in Fig 3a). Finally, we notice the existence of a region of suppressed or weakly reversed current for stronger driving and intermediate interaction.

Figure 4a shows the effect of departing from exact resonance. In general, the effect of $\Delta > 0$ is that of shifting the behavior of current towards higher interactions. In particular, we note that, starting from the white-blue region of suppressed or reversed current, interactions tend to restore the positive ratchet current. This effect can be understood if one notes that, for positive detuning, the effective degeneracy between the three states $\pm, 0$ disappears because $|0\rangle$ acquires a higher energy. Degeneracy is restored due to the massive initial occupation of $|0\rangle$, which lowers its energy via the attractive mean-field interaction in (10). It thus becomes clear that the effect of a positive detuning is counteracted by an increase of the effective attraction. In particular, the starting degeneracy recovered with the help of interactions permits the onset of Rabi oscillations known to be essential for the emergence of a ratchet current [14].

Figure 3b shows the population of the third eigenstate of the one-particle density matrix, n_3 . Comparison with Fig. 3a shows a clear correlation between the occupation of a third state and the suppression or weak reversal of

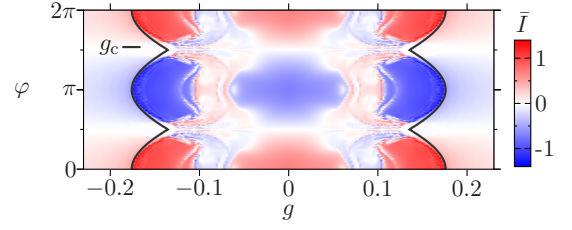


FIG. 5. *Current dependence on φ .* Ratchet current in 3GP as a function of the phase φ and the interaction strength g . Parameters: $\omega = 1$ ($\Delta = 0$), $K = 0.2$, $\alpha = \beta = 0.2$. Averages are performed over 400 cycles.

the ratchet current. The dynamics of a macroscopic condensate in a three-level system is that of two coupled non-rigid pendula, which beyond the harmonic regime can be expected to be chaotic. This behavior is confirmed from the inspection of Figs. 4b-f. In Fig. 4b we show a plot of \bar{I} as a function of Δ for a particular value of g , obtained with the three different calculation methods described above. For the values of Δ marked with labels c-f, we show in Figs. 4c-f the corresponding Poincaré cross sections. The one point which shows chaotic behavior is e, which falls in the white-blue region of Fig. 4a. We have just noted (see Fig. 3a) that such a region is correlated with the occupation of a third eigenstate and thus with the possible emergence of chaotic behavior on the coarse-grained time scale. This underlines the connection between three-level occupation, chaotic behavior, and current reduction or reversal.

Figure 4b also indicates that in the chaotic regime the convergence in time is slower than in the regular regime, as can be seen by the discrepancy between 3GP calculations performed over 400 or 10^4 driving periods. We emphasize that the current reversal feature in the chaotic region is not just a transient but reflects a lasting behavior; we have checked it up to 10^5 periods in some cases. Finally, we note that all calculations made in the FGP approximation indicate that, for large K and g close to the self-trapping transition g_c (beyond which only the state $|0\rangle$ intervenes), the behavior has an important influence from states beyond the three-state basis $0, \pm$ (not shown).

In Fig. 5 we show how the the ratchet current depends on the choice of initial driving phase. A change $\varphi = 0 \rightarrow \pi$ corresponds to $K \rightarrow -K$ and thus to a reversal of the current. On the other hand, we note that for $\varphi = \frac{1}{2}\pi, \frac{3}{2}\pi$ the ratchet current is always zero, because parity is restored for those values of φ . Figure 5 also shows that the long time averaged current (but not the instantaneous one) is an even function of the interaction strength.

In summary, we have introduced a formalism to account for interactions in ac-driven many-body systems. In the case where only resonant states effectively inter-

vene, we derive a Hamiltonian involving conventional operators which describes the long time dynamics of the driven system. We have applied the method to the calculation of the coherent ratchet current carried by an asymmetrically driven atomic condensate and compared it with continuum and truncated mean-field descriptions. We have found a rich dynamical behavior with crossovers from self-trapping to regular oscillations to chaotic behavior.

We thank Justin Anderson for useful discussions. The authors acknowledge support from the MICINN through Grant No. FIS2010-21372 and the Ramón y Cajal program (CEC), the Comunidad de Madrid through Grant Microseres, the Heidelberg Center for Quantum Dynamics, and the NSF.

-
- [1] B. D. Josephson, *Phys. Lett.* **7**, 251–253 (1962).
 - [2] P. W. Anderson, J. M. Rowell, *Phys. Rev. Lett.* **10** 230–232 (1963); S. Shapiro, *Phys. Rev. Lett.* **11** 80–82 (1963).
 - [3] O. Avenel and E. Varoquaux, *Phys. Rev. Lett.* **55** 2704–2707 (1985).
 - [4] D. S. Hall, M. R. Matthews, C. E. Wieman, E. A. Cornell, *Phys. Rev. Lett.* **81**, 1543–1546 (1998).
 - [5] T. Zibold, E. Nicklas, C. Gross, and M. K. Oberthaler, *Phys. Rev. Lett.* **105**, 204101 (2010).
 - [6] M. Albiez, R. Gati, J. Fölling, S. Hunsmann, M. Cristiani, and M. K. Oberthaler, *Phys. Rev. Lett.* **95**, 010402 (2005).
 - [7] A. Micheli, D. Jaksch, J. I. Cirac, and P. Zoller, *Phys. Rev. A* **67** 013607 (2003).
 - [8] I. Zapata, F. Sols, A. J. Leggett, *Phys. Rev. A* **57**, R28–R31 (1998).
 - [9] F. Sols, in *Bose-Einstein Condensation in Atomic Gases*, edited by M. Inguscio, S. Stringari, and C. E. Wieman (IOS Press, Amsterdam, 1999).
 - [10] M. Holthaus, *Phys. Rev. A* **64**, 011601 (2001).
 - [11] S. Denisov, L. Morales-Molina, S. Flach, and P. Hänggi, *Phys. Rev. A* **75**, 063424 (2007).
 - [12] C. E. Creffield and F. Sols, *Phys. Rev. Lett.* **103**, 200601 (2009).
 - [13] S. Wüster, B. J. Dabrowska, M. J. Davis, *arXiv:1112.2086* (2011).
 - [14] M. Heimsoth, C. E. Creffield, and F. Sols, *Phys. Rev. A* **82**, 023607 (2010).
 - [15] J. Santos, R. A. Molina, J. Ortigoso, and M. Rodríguez, *Phys. Rev. A* **84** 023614 (2011).
 - [16] A. S. Arnold, C. S. Garvie, and E. Riis, *Phys. Rev. A* **73** 041606 (2006); S. R. Muniz, S. D. Jenkins, T. A. B. Kennedy, D. S. Naik, and C. Raman, *Opt. Express* **14** 8947–8957 (2006); C. Ryu, M. F. Andersen, P. Cladé, V. Natarajan, K. Helmerson, W. D. Phillips, *Phys. Rev. Lett.* **99**, 260401 (2007); K. Henderson, C. Ryu, C. MacCormick, and M. G. Boshier, *New J. Phys.* **11** 043030 (2009); S. Moulder, S. Beattie, R. P. Smith, N. Tammuz, and Z. Hadzibabic, *arXiv:1112.0334* (2011).
 - [17] J. S. Howland, *Math. Ann.* **207**, 315–335 (1974).
 - [18] A. J. Leggett, *Quantum Liquids*, 1st edition, chapter 2.3 (Oxford University Press, 2006).
 - [19] T. Salger, S. Kling, T. Hecking, C. Geckeler, L. Morales-Molina, and M. Weitz, *Science* **326**, 1241 (2009).
 - [20] S. Kohler and F. Sols, *Phys. Rev. Lett.* **89**, 060403 (2002).
 - [21] A. Smerzi, S. Fantoni, S. Giovanazzi, and S. R. Shenoy, *Phys. Rev. Lett.* **79**, 4950 (1997).